Colloids and Surfaces A: Physicochemical and Engineering Aspects 653 (2022) 129943

Contents lists available at ScienceDirect

Colloids and Surfaces A: Physicochemical and Engineering Aspects

journal homepage: www.elsevier.com/locate/colsurfa

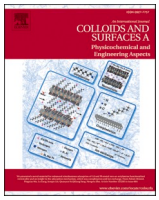

Hydration and antibiofouling of TMAO-derived zwitterionic polymers surfaces studied with atomistic molecular dynamics simulations

Pranab Sarker [a], Grace Tang Chen [b], Md Symon Jahan Sajib [a], Nathan Wesley Jones [c], Tao Wei [a,*]

[a] Department of Chemical Engineering, Howard University, Washington, D.C. 20059, USA
[b] Adlai E. Stevenson High School, Lincolnshire, IL 60069, USA
[c] Crayton Pruitt Family Department of Biomedical Engineering, University of Florida, Gainesville, FL 32612, USA

HIGHLIGHTS

- Atomistic molecular dynamics simulations of TMAO-derived polymer surfaces' antibifouling.
- Condensed and ordered hydration layer on the polymer surfaces.
- Hydration free energy barrier to resist protein adsorption.

GRAPHICAL ABSTRACT

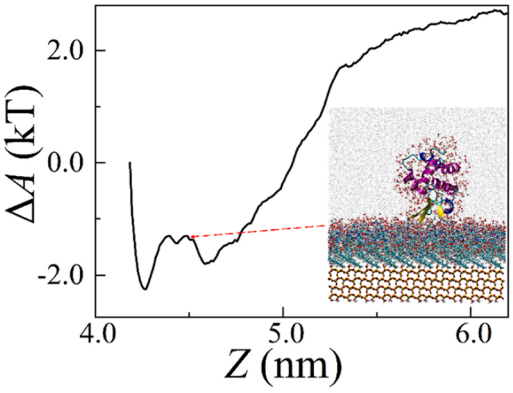

ARTICLE INFO

Keywords:
Antibiofouling
Hydration
TMAO Surfaces
MD Simulations
Desorption Free Energy

ABSTRACT

Zwitterionic polymers have emerged as a class of highly effective ultralow fouling materials for critical marine coating and biomedical applications. The recently developed trimethylamine N-oxide (TMAO)-derived zwitterionic polymers have demonstrated excellent antibiofouling capability in various chemical environments; however, it remains unclear how they interact with proteins at the microscopic level. To further investigate the antifouling mechanisms, we performed atomistic molecular dynamics (MD) simulations in combination with free-energy computations to provide an in-depth molecular understanding of the interactions of TMAO polymer brush (pTMAO) surfaces with proteins of opposite charges (positively charged lysozyme and negatively charged barnacle cement protein) in aqueous environments (pure water and saline solution). Our simulations revealed ordered structures of a condensed hydration water layer on the pTMAO surfaces in pure and saline water. The quantitative free energy analyses showed that the pTMAO surface has small protein desorption energy, but with a strong hydration energy barrier near the polymer surfaces to resist protein adsorption compared to other biofouling surfaces. The addition of salts only has a slight effect on the pTMAO surface's exclusion of proteins due to the small interference of the structure of interfacial water. This study provides detailed knowledge of the

* Corresponding author.
E-mail address: tao.wei@howard.edu (T. Wei).

https://doi.org/10.1016/j.colsurfa.2022.129943
Received 26 July 2022; Received in revised form 10 August 2022; Accepted 10 August 2022
Available online 19 August 2022

strong surface hydration of zwitterionic polymers and its relation to salt impact, protein adsorption, and antibiofouling behavior of these important materials.

1. Introduction

Biofouling occurs through the attachment of biomolecules and other biological materials/systems onto surfaces. For example, marine biofouling can be caused by adsorption of proteins or microorganisms, such as bacteria, mussels, barnacles, algae and seaweed, onto ship hulls, which gives rise to an increase in the hydrodynamic drag on vessels' sailing, while also leading to pitting and crevice corrosion of vessels' metal surfaces [1,2]. Efforts to control marine biofouling cost governments and industries around the world billions of dollars annually [3]. For example, biofouling costs the US Navy hundreds of million dollars for the maintenance of battle ships [4]. Biofouling is a successional process, with the settlement (attachment) and growth of biofoulers including four steps: conditioning with proteins/carbohydrates, soft microfouler settlement and biofilm formation, soft macrofouler settlement, and finally, hard fouler settlement [5]. A small amount of proteins (< 5 ng cm^{-2}) adsorbed on the surface can introduce multilayer protein adsorption and the propagation of biofouling [6–8]. Biofouling-resistant coating materials based on toxic biocide-containing paints, e.g., tributyl tin-, and copper- and zinc-based biocides, can cause environmental contamination [5,9,10]. New environmentally benign fouling-resistant coating materials are highly desired. The fundamental studies of biofouling/antibiofouling impact not only marine applications [11] and biomaterials [12], but also many applications in other areas such as the food industry [13], membrane separation [14–16] and beyond. Thus it is important to study biofouling mechanisms and strategies to control or minimize biofouling.

Zwitterionic materials, which contain an equal number of oppositely charged moieties with a net neutral charge, have emerged as a class of highly effective ultralow fouling biomedical and engineering materials [7,17]. Due to the electrostatically induced hydration layer, surfaces coated with zwitterionic polymers exhibit strong resistance to nonspecific protein adsorption (<3 ng cm^{-2}), bacterial adhesion, and biofilm formation [7,17–20]. These zwitterionic polymers also possess other desirable properties for practical applications, such as ease of preparation, chemical stability, and low cost [7]. The zwitterionic materials currently available include poly(phosphorylcholine) (pPC), which mimics zwitterionic phosphorylcholine moieties' outer cell membranes; [21] poly(sulfobetaine) (pSB) derived from taurine; [22] poly(carboxybetaine) (pCB) derived from glycine betaine; [23] and the newly developed trimethylamine N-oxide (TMAO)-derived zwitterionic polymers (pTMAO) [17]. The experimental rule of thumb is that the antibiofouling property of zwitterionic polymers increases as the spacing decreases between the positively and negatively charged sites of zwitterionic moieties [7,17,24]. Experiments show that pTMAO consists of monomers with directly connected oppositely charged moieties (Me_3N^+-O^-) [17,25], which display excellent salt resistance and antibiofouling due to strong surface hydration [26].

Atomistic molecular dynamics (MD) simulations have been extensively applied to the study of protein's interfacial behavior on surfaces in explicit water with atomistic accuracy [26–35]. Simulation studies show that on fouling surfaces, protein adsorption can be divided into three stages: diffusion onto the surface, dehydration induced by surface-protein interactions, and protein structural denaturation [28,32]. Slow dehydration of the interfacial water leads to the protein's structural deformation and stronger adsorption on the substrate surface [28]. Extensive simulation studies [36–41] have also been done to probe the interactions of zwitterion with protein, water, and electrolytes in the solution environment. Polymer surfaces' hydrophobicity, interfacial hydration, and morphology are important to their interactions with biofoulers, such as the adsorbed protein's structure and mobility [15,26,27]. To the best of our knowledge, it remains unclear how zwitterionic polymer surfaces interact with proteins at the polymer-water interface at the atomistic and molecular scales.

In this study, atomistic MD simulations were performed to provide quantitative free energy analyses of the interactions of pTMAO brush surfaces with proteins and salts. Positively charged lysozyme protein (pdb: 1HWA) and negatively charged barnacle cement protein MrCP20 (pdb: 6LEK) at pH 7 were chosen to study their interactions with pTMAO surfaces in this work. In addition to their different charges, we chose those two proteins for study because (1) we have previously studied lysozyme adsorption on many surfaces [1,15,27–29,42,43], and, therefore, lysozyme adsorption on pTMAO will provide us with unique knowledge of the similarities and differences between protein adsorption on zwitterionic polymer surfaces and other surfaces; (2) barnacle cement protein MrCP20 is one of the primary proteins that constitute adhesive cement in *Megabalanus rosa*, a commonly investigated barnacle species [44]. Protein MrCP20 enables barnacles to remain well adhered to surfaces submerged in water because of its charged functional group, which allows for multiple attachment sites, promoting fixation to the substrate, biomineralization control, and inhibition of calcium carbonate formation [45]. Barnacle protein MrCP20 serves as a great model for adhesive proteins – an investigation of barnacle protein–pTMAO surface interaction will lead to a crucial understanding of the antifouling mechanisms of zwitterionic polymers. We focused on the effects of polymer surfaces' hydration on protein–surface interaction, as it is the key factor for the zwitterionic pTMAO polymer surfaces' antibiofouling functionalities. It is worth mentioning that despite our previous study of lysozyme interactions with pTMAO polymer surfaces of larger TMAO terminal groups in 0.6 M salt solution previously [27], detailed salt effects on such interactions, quantitative free energy analyses, and the comparisons between pTMAO and other surfaces have not been reported, which are crucial for understanding the excellent antifouling performance and unique strong resistance against salt disruption on the surface hydration of pTMAO.

2. Methodology

The atomistic MD simulations were performed using the software of GROMACS [46] (version 2019.6) with the CHARMM36 force field [47] and the TIP3P water model. The pTMAO brush surface was designed by connecting four TMAO brushes with a hydroxylated α-cristobalite (101) crystal unit. Each TMAO brush has a terminal group containing the TMAO functionality (i.e., the TMAO repeating unit $n = 1$) and is connected to the surface with an alkyl spacer, $-(CH_2)_{10}$ with the packing density of 2.4 chains/nm^2. The entire pTMAO brush surface was prepared by the periodical expansion of the above surface unit along the *X*- and *Y*- directions (Fig. 1). The positions of atoms of the α-cristobalite (101) surface were fixed during the simulation. An implicit wall of repulsive Lennard–Jones potential at the top of the simulation box was used to prevent the diffusion of water molecules in the *Z*- direction (Fig. 1). The charges for pTMAO chains were obtained from our previous quantum computation [26], and those for the hydroxylated α-cristobalite substrate were adopted from the literature [27,48]. The system was maintained at a temperature of 298.15 K using the thermostat method of modified Berendsen [49]. To estimate the protein surface's binding affinity, the potential of mean force for the protein-surface interactions and protein desorption free energy ΔA were measured using nonequilibrium steered molecular dynamics (SMD) [50] simulations and weighted histogram analysis (WHAM) [51] of the probability histograms generated from a series of umbrella sampling simulations. Due to the nature of the antibiofouling of the pTMAO surface, we directly

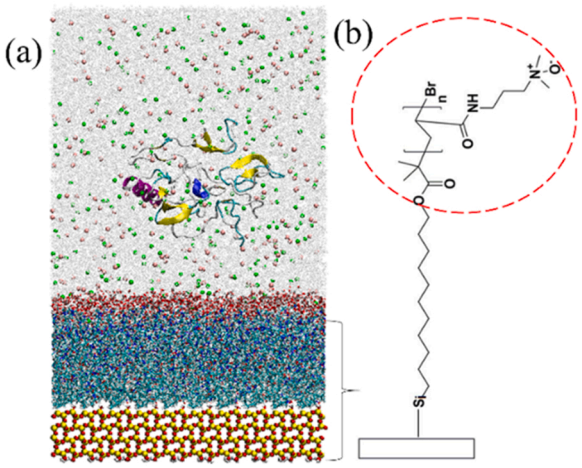

Fig. 1. (a) Snapshot of the simulation system of barnacle cement protein (pdb: 6LEK) on pTMAO surfaces and (b) the schematics of the unit cells of α-cristobalite (101) surface modified by TMAO monomers (red cycle). The packing density of pTMAO is 2.4 chains/nm^2 and the number of repeating units (n) of the TMAO terminal group is 1. Atoms in the system are shown in yellow (silicon), red (oxygen), white (hydrogen), gray (bulk water), green (Cl^-) and orange (Na^+). The interfacial water on the pTMAO brush surface is highlighted with red color. Implicit walls with repulsion forces are applied on the top and bottom of the simulation box to enclose the entire system. The interfacial water above pTMAO surfaces are colored red.

placed the protein on the pTMAO surfaces and then pulled the protein away at different gapping distances to the surface for further WHAM analyses. More details of the simulation and desorption free energy computation are shown in the Supplementary material.

3. Results and discussion

3.1. Interactions between positively charged lysozyme and pTMAO surface

To examine protein-surface interactions during adsorption, we first adopted the positively charged lysozyme protein (+8e) in water at pH 7 and measured the potential of mean force (PMF) for the protein desorption to quantify its desorption free energy ΔA on the hydrophilic pTMAO surfaces for comparison with the hydrophobic azobenzene–terminated surfaces, which was published in our previous study [27]. It is worth noting that both surfaces contain the same α-cristobalite substrate grafted with identical alkyl spacers, $-(CH_2)_{10}$ and the same surface packing densities, except for the difference in terminal groups. Even though we used a small terminal unit of TMAO (the repeating unit, $n = 1$) for each chain in this study, our simulations of 200 ns showed that the lysozyme cannot adsorb onto the pTMAO surface while it has a large degree of rotations, which is similar to that of pTMAO surfaces with large TMAO terminal units ($n = 4$) in our previous study [26]. But this is totally different from the rapid protein adsorption on other biofouling surfaces, such as the azobenzene-terminated brush surface [27], polyethylene surfaces [28], polyamide membrane [15], graphene [1,52], gold surface [42] and metal nanoparticles [43,53].

To measure the strength of the interactions of lysozyme-pTMAO surfaces, we artificially placed a lysozyme protein on the surface to estimate the protein desorption free energy ΔA using the profile of potential of mean force (PMF) of protein desorption. Our computation shows that ΔA is only 4.0 kT on pTMAO surfaces in pure water, which is one order of magnitude lower than that on a *trans*-azobenzene-terminated surface (60 kT) [48] in the same aqueous environment. This suggests that the TMAO-terminated surface is antibiofouling, whereas the *trans*-azobenzene-terminated surface is biofouling. It is worth noting that for both cases, a bump in the desorption free energy profiles is observed at ~3 Å above the top of the pTMAO surface, which serves as an energy barrier for the protein's landing (Fig. 2). The small energy barrier of the hydrophobic *trans*-azobenzene-terminated surfaces results mainly from protein hydration, which was detected in the neutral scattering experiments [54] and atomistic MD simulations [1,28,29]. Due to the protein's surface charges and hydrophilic residues on the protein surface, a protein molecule is surrounded by a condensed hydration layer [1,28,29,54]. The *trans*-azobenzene-terminated surface is also covered with hydration water. Upon protein adsorption, the interfacial water between the protein and the surface needs to be depleted. However, on the antibiofouling pTMAO surfaces, the energy barrier at $z = 4.2$–4.5 nm is larger than that of the biofouling azobenzene surface, which is mainly due to the protein surface's hydration and the strong hydration of pTMAO surfaces, which will be discussed later. Therefore, it is much more difficult for the lysozyme to be adsorbed onto the pTMAO surface. It is worth noting that the hydration energy barrier at the substrate surface-water interface of protein/peptide adsorption is visible on the PMF curves for other surfaces regardless of their hydrophobicity and biofouling/antibiofouling properties, e.g., cardiotoxin protein on a methyl-terminated self-assembled monolayer (SAM) [55], lysozyme on an Au(111) surface [56], and tripeptide on hydroxyapatite [57]. Additionally, the hydration barrier is discernible in the cases of ligand adsorption on biomolecule surfaces, e.g., levodopa into β-cyclodextrin [58], and metalloproteinase-9 and the linking peptide of activatable cell-penetrating peptide [59]. However, in those previous studies [55–59], the sophisticated feature of the PMF profile, i.e., a free energy bump on the PMF above the surface at ~3 Å, was generally ignored, without further discussion of its correlation with interfacial hydration.

Since zwitterionic polymers are targeted for use in contact with blood/tissue (as biomaterials) or in the marine environment (as antifouling coatings for marine vessels), and both blood/tissue and seawater have high salt contents, it is necessary to study the salt effect on the protein–surface interactions. To study the salts' effect on the interactions of pTMAO with the lysozyme protein, we measured the lysozyme protein desorption free energy by using the same initial configuration, i.e., the same protein's structure and orientation on the pTMAO surface in the 0.6 M NaCl solution, as the ionic strength of sea water is around 0.6 M. Fig. 3 shows that the desorption free energy ΔA slightly increases to 4.96 kT in saline water. The small increase in ΔA (~1 kT) in saline water compared to that of pure water indicates that the addition of salts slightly decreases pTMAO surface hydration and antibiofouling capability. Moreover, our simulations show that the protein's orientations on pTMAO surfaces largely vary at different gapping distances to the surfaces, particularly around the area of the hydration energy barrier at $Z \sim 4.25$–4.55 nm (see snapshots in Fig. 3), which can be attributed to the surface hydration barrier. Nevertheless, the addition of salt only slightly impacts lysozyme–surface interactions for pTMAO, which is still markedly different from the lysozyme–surface interactions of other materials previously studied, e.g., aromatic polyamide membrane [14,15], polyethylene glycol [60] and phosphorylcholine [60]. This study shows that the surface hydration of pTMAO remains high even in a high salt solution (0.6 M), ensuring the excellent antifouling performance of pTMAO in different environments.

3.2. Structure and hydration of pTMAO surfaces

To further understand the slightly different lysozyme–pTMAO interactions in the cases of pure water and 0.6 M NaCl solution, we also studied the effects of salt on the pTMAO structure. The density profiles of TMAO terminals and the alkyl spacer linkage in both pure water and saline water show that the hydrophilic TMAO terminal groups are located above the alkyl chains and are exposed to the bulk water environment (Fig. 4a). The negligible difference in the density profiles, typically at the polymer–water interface, suggests a slight salt effect on the polymer chain packing, which is well correlated to the slight salt

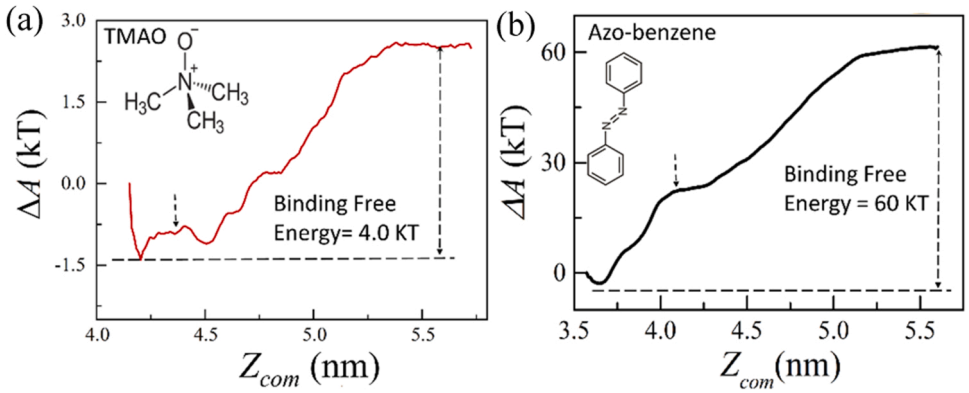

Fig. 2. Desorption free energy, Δ*A*, of a lysozyme protein (pdb: 1HWA) as a function of the position of the protein's center of the mass (Z_{com}) along the *Z*-axis: (a) pTMAO brush surfaces and (b) *trans*-azobenzene-terminated brush surfaces in pure water. The energy barrier on both surfaces is indicated by an arrow. Fig. 2b is adapted with permission from ref 27. Copyright 2016 American Chemical Society.

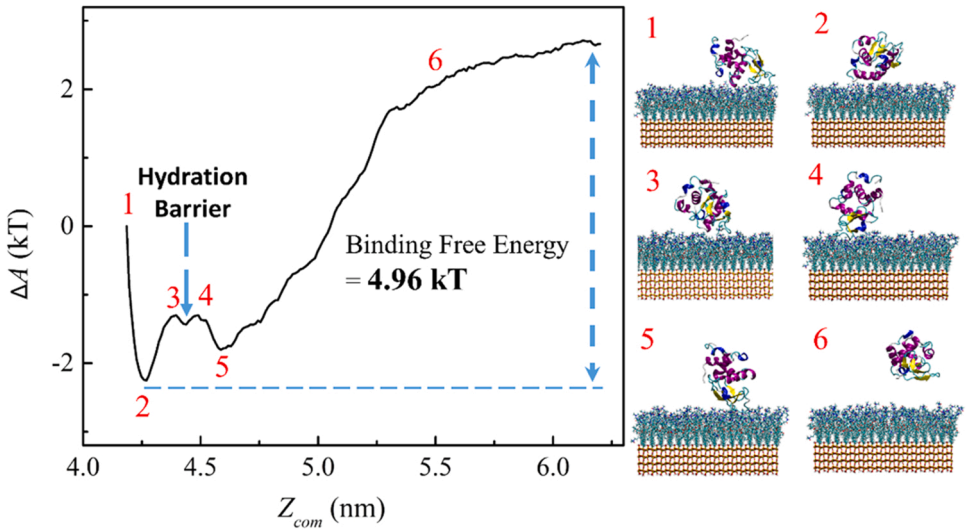

Fig. 3. Desorption free energy, Δ*A* of a lysozyme protein (pdb: 1HWA) as a function of the position of the protein's center of the mass (Z_{com}) along the *Z*-axis on the pTMAO brush surfaces in the 0.6 M NaCl solution and the corresponding snapshots.

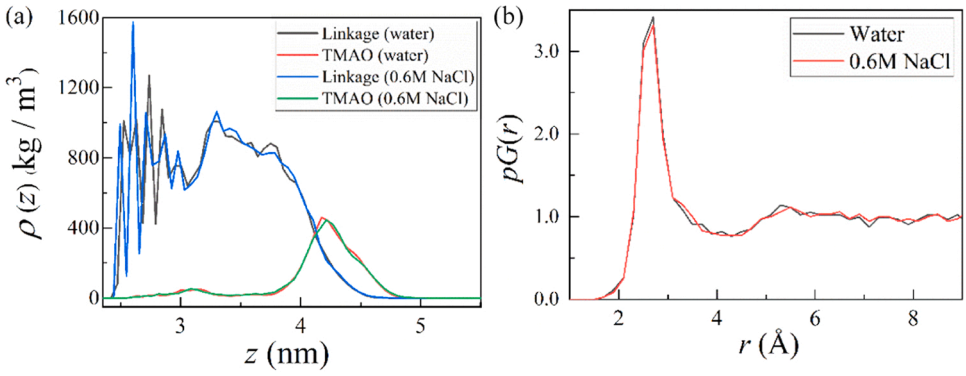

Fig. 4. Comparison of the cases in pure water and 0.6 M NaCl solution: (a) density profile ρ (z) of the alkyl linkages and TMAO terminals along the surface normal (i.e., the *Z*-axis); (b) proximal radial distribution function *pG(r)* of the surface hydration density profiles. Twenty configurations were obtained in the last 5 ns after a relaxation of 30 ns by constraining the center of the mass of the protein with the protein's minimum surface distance $d \geq 1.2$ nm, which eliminates the surface-surface interaction. A lysozyme protein is located at $Z \sim 6.0$–9.3 nm in the bulk. The density profile ρ (z) was computed using the mass divided by the total volume without incorporating the exclusion volume of polymers.

effect on lysozyme–pTMAO interactions in the two cases. We also examined the salt effect on the distribution of oxygen and nitrogen. For the pTMAO surfaces with small terminal units of TMAO (i.e., repeating unit $n = 1$), negligible differences were detected in the number densities of nitrogen and oxygen atoms in both cases of pure water and 0.6 M NaCl (Fig. S1 in the Supplementary material). To analyze water distribution near the amorphous pTMAO surface, we computed the normalized water concentration, referring to the bulk water density using the proximal radial distribution function *pG(r)* [28], where *r* is the minimum distance of a water oxygen atom to the pTMAO brush surface's atoms. Similar to our previous study of pTMAO with a large repeating unit of TMAO ($n = 4$) and experimental measurement [26], our *pG(r)* shows that the pTMAO surface with the TMAO repeating unit ($n = 1$) is covered with a very condensed hydration layer (Fig. 4b and

Fig. 1). The addition of the salts leads to a very slight reduction of the pTMAO surface hydration density (Fig. 4b). Both Na^+ cations and Cl^- anions are screened away from the polymer surfaces (Fig. S2 in the Supplementary material).

The distribution of water orientations is analyzed using two-dimensional orientational distribution [61] (Fig. 5a,b)

$$\omega(z,\ \theta) = \frac{\langle \delta(\theta - \theta(t))\delta(z - z(t))\rangle}{\omega_0 \rho(z)\sin(\theta)} \quad (1)$$

where z is the coordinate along the surface normal pointing to the bulk water; θ represents an angle between the dipole vector of water and the Z-axis; ρ (z) is the local water density at z; $sin(\theta)$ is the angular Jacobian factor and ω_0 is the averaged bulk value of orientational distribution for normalization. In consistence with the hydration energy barrier of the desorption free energy ΔA (Figs. 2a and 3) and TMAO density profile (Fig. 4a), the profiles of $\omega(z,\theta)$ in both cases of pure water and 0.6 M salt solution show that most water molecules have θ ~130–180 ° at the pTMAO polymers-water interface (z = 4.1–4.5 nm) (Fig. 5a, b, c). Those interfacial water molecules form hydrogen bonds with the TMAO oxygen atoms or have non-hydrogen bonding interactions with TMAO (Fig. 5c). To quantify the ordering of interfacial water molecules, we used the order parameter, S, defined at different locations along the Z-axis direction,

$$S(z) = \left\langle \frac{3cos^2(\theta(z)) - 1}{2} \right\rangle \quad (2)$$

Fig. 5d shows that interfacial water molecules exhibit ordered structure in both cases of pure water and 0.6 M NaCl. However, the addition of salts slightly altered the ordering of the interfacial water molecules, leading to a small difference in the protein desorption free energy (Fig. 3). Despite the presence of the lysozyme in the bulk (at Z ~ 6.0–9.3 nm), water molecules are generally disordered in this bulk area (Fig. 5**a, b, d**).

3.3. *Interactions between negatively charged barnacle cement protein and pTMAO surface*

To further study the pTMAO surface's antibiofouling functionality, we also adopted a negatively charged barnacle cement MrCP20 protein (−26*e*). Barnacle attachment, which involves barnacle cement protein–surface interaction, has been extensively used to test the biofouling and antifouling performance of coating materials [2,62]. Similar to the interfacial behavior of an oppositely charged lysozyme protein, a barnacle protein cannot adsorb on TMAO brush surfaces in 0.6 M salt solution without an external constraint force applied (see Movie 1 in Supplementary material). The barnacle protein rotates and bumps on pTMAO surfaces. We also used the same simulation protocol by artificially placing the barnacle protein on pTMAO brush surfaces to measure the strength of protein-surface interactions. Our computations showed that despite the large size and molecular weight of a barnacle protein, the desorption free energy ΔA is still small (~18.5 kT) (Fig. 6). However, the ΔA profile of barnacle is less smooth than that of lysozyme (Figs. 3, 6) due to the highly non-spherical shape of the barnacle protein. The large-degree rotation of a barnacle at different gapping distances from the protein's center of the mass to the top of pTMAO surfaces introduces multiple points of contact of the barnacle protein with the pTMAO surfaces, leading to multiple transitions of the desorption free energy

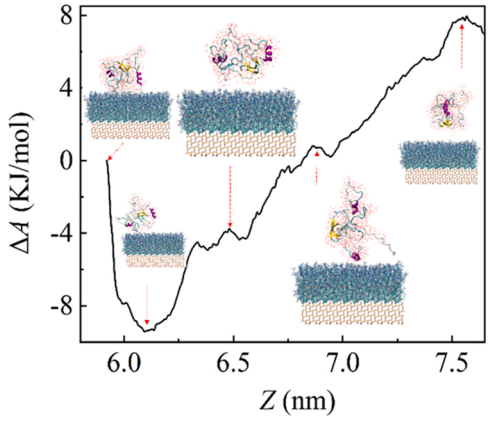

Fig. 6. Desorption free energy, ΔA, of a barnacle cement MrCP20 protein (pdb: 6LEK) as a function of the position of the protein's center of the mass (Z_{com}) along the Z-axis on the pTMAO brush surfaces in the 0.6 M salt solution and the corresponding snapshots.

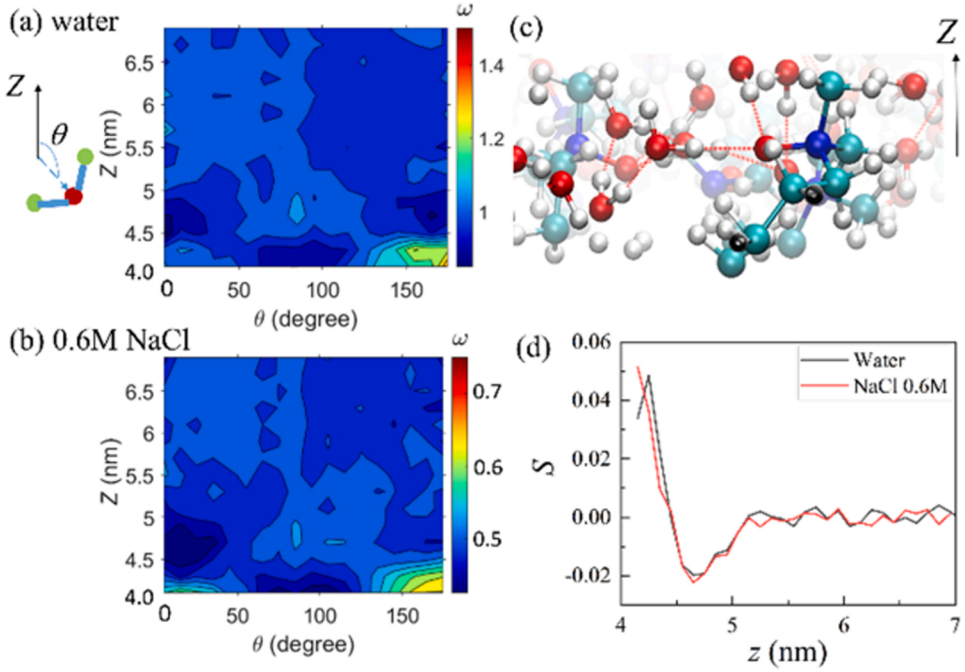

Fig. 5. Two-dimensional orientational distribution $\omega(z,\theta)$ of water molecules in the cases of pure water (a) and 0.6 M NaCl solution (b); a snapshot at the pTMAO surface-water interface (z = 4.0–4.3 nm) in the case of pure water (hydrogen bonds are represented by the red dash line) (c); and order parameter profile S along the Z-axis. To compute the $\omega(z,\theta)$ profiles, 200 configurations were obtained in the last 5 ns after 30-ns relaxation. To eliminate the surface-surface interactions, the center of the mass of the protein was constrained in the bulk with the protein's minimum surface distance $d \geq 1.2$ nm during relaxation. A lysozyme protein is located at Z ~ 6.0–9.3 nm in the bulk. The bulk value of ω_0 at z = 12–13 nm (far away from the protein and the pTMAO surface) was used for normalization.

profile of the barnacle cement MrCP20 protein.

Supplementary material related to this article can be found online at doi:10.1016/j.colsurfa.2022.129943.

4. Conclusions

In this work, we studied the interactions of zwitterionic pTMAO surfaces with oppositely charged proteins in pure water and saline water using atomistic MD simulations and free energy computation. Our study, for the first time, quantitatively demonstrated that the interfacial hydration free energy barrier for pTMAO surfaces, which elucidates the surface's antibiofouling mechanism. The small protein desorption free energy and the protein's large interfacial mobility, regardless of the difference in the charges and the size of proteins, demonstrates the outstanding antibiofouling functionality of pTMAO surfaces compared with the biofouling properties of azobenzene-terminated brush surfaces. Moreover, our analyses showed that the pTMAO surface is covered with a condensed and ordered layer of interfacial water, which is responsible for the hydration energy barrier for protein adsorption near the surface and the polymer surface's super resistance to protein adsorption. The addition of salts has a small effect on the surface's hydration and antibiofouling. Our fundamental study of the interfacial behavior of TMAO-derived zwitterionic polymers at the atomistic scale will be critical to the future development of zwitterionic materials for applications in the marine vessel and biomedical industries.

Supplementary material

Details of the atomistic simulations and desorption free energy computations, the density distribution of nitrogen and oxygen of pTMAO on the surface. Figure of oxygen and nitrogen atoms' distribution on pTMAO surface in pure water and 0.6 M NaCl. Movie of a barnacle cement protein MrCP20 on pTMAO brush surfaces in 0.6 NaCl (AVI). Movie showing the protein interfacial behavior and pTMAO surface's antibiofouling.

CRediT authorship contribution statement

All listed authors have equal contributions to conceptualization, methodology, formal analysis, validation and manuscript writing of this work.

Declaration of Competing Interest

The authors declare that they have no known competing financial interests or personal relationships that could have appeared to influence the work reported in this paper.

Data availability

No data was used for the research described in the article.

Acknowledgments

TW acknowledges the grant support from the Office of Naval Research Award N00014-21-1-2215. TW is indebted to the grant support of computational resources at the program of Extreme Science and Engineering Discovery Environment (XSEDE) and the Texas Advanced Computing Center (TACC).

Appendix A. Supporting information

Supplementary data associated with this article can be found in the online version at doi:10.1016/j.colsurfa.2022.129943.

References

[1] C.M. Nakano, H. Ma, T. Wei, Study of lysozyme mobility and binding free energy during adsorption on a graphene surface, Appl. Phys. Lett. 106 (2015), 153701.
[2] C.R. So, E.A. Yates, L.A. Estrella, K.P. Fears, A.M. Schenck, C.M. Yip, K.J. Wahl, Molecular recognition of structures is key in the polymerization of patterned barnacle adhesive sequences, ACS Nano 13 (2019) 5172–5183.
[3] J. Bellas, Comparative toxicity and of alternative antifouling biocides on embryos larvae of marine invertebrates, Sci. Total Environ. 367 (2006) 573–585.
[4] M. Schultz, J. Bendick, E. Holm, W. Hertel, Economic impact of biofouling on a naval surface ship, Biofouling 27 (2011) 87–98.
[5] A.K. Leonardi, C.K. Ober, Polymer-based marine antifouling and fouling release surfaces: strategies for synthesis and modification, Annu. Rev. Chem. Biomol. Eng. 10 (2019) 241–264.
[6] W.B. Tsai, J.M. Grunkemeier, T.A. Horbett, Human plasma fibrinogen adsorption and platelet adhesion to polystyrene, J. Biomed. Mater. Res. 44 (1999) 130–139.
[7] S. Jiang, Z. Cao, Ultralow-fouling, functionalizable, and hydrolyzable zwitterionic materials and their derivatives for biological applications, Adv. Mater. 22 (2010) 920–932.
[8] T. Wei, S. Kaewtathip, K. Shing, Buffer effect on protein adsorption at liquid/solid interface, J. Phys. Chem. C 113 (2009) 2053–2062.
[9] L.D. Chambers, K.R. Stokes, F.C. Walsh, R.J. Wood, Modern approaches to marine antifouling coatings, Surf. Coat. Technol. 201 (2006) 3642–3652.
[10] A. Turner, Marine pollution from antifouling paint particles, Mar. Pollut. Bull. 60 (2010) 159–171.
[11] I. Fitridge, T. Dempster, J. Guenther, R. De Nys, The impact and control of biofouling in marine aquaculture: a review, Biofouling 28 (2012) 649–669.
[12] W. Yang, L. Zhang, S. Wang, A.D. White, S. Jiang, Functionalizable and ultra stable nanoparticles coated with zwitterionic poly (carboxybetaine) in undiluted blood serum, Biomaterials 30 (2009) 5617–5621.
[13] J. Verran, Biofouling in food processing: biofilm or biotransfer potential? Food Bioprod. Process. 80 (2002) 292–298.
[14] J. Wang, Z. Wang, J. Wang, S. Wang, Improving the water flux and bio-fouling resistance of reverse osmosis (RO) membrane through surface modification by zwitterionic polymer, J. Membr. Sci. 493 (2015) 188–199.
[15] M.S. Jahan Sajib, Y. Wei, A. Mishra, L. Zhang, K.-I. Nomura, R.K. Kalia, P. Vashishta, A. Nakano, S. Murad, T. Wei, Atomistic simulations of biofouling and molecular transfer of a cross-linked aromatic polyamide membrane for desalination, Langmuir 36 (2020) 7658–7668.
[16] T.A. Desai, D.J. Hansford, L. Leoni, M. Essenpreis, M. Ferrari, Nanoporous anti-fouling silicon membranes for biosensor applications, Biosens. Bioelectron. 15 (2000) 453–462.
[17] B. Li, P. Jain, J. Ma, J.K. Smith, Z. Yuan, H.-C. Hung, Y. He, X. Lin, K. Wu, J. Pfaendtner, S. Jiang, Trimethylamine N-oxide–derived zwitterionic polymers: a new class of ultralow fouling bioinspired materials, Sci. Adv. 5 (2019) eaaw9562.
[18] S. Chen, L. Li, C. Zhao, J. Zheng, Surface hydration: principles and applications toward low-fouling/nonfouling biomaterials, Polymer 51 (2010) 5283–5293.
[19] C. Leng, S. Sun, K. Zhang, S. Jiang, Z. Chen, Molecular level studies on interfacial hydration of zwitterionic and other antifouling polymers in situ, Acta Biomater. 40 (2016) 6–15.
[20] C. Leng, H.-C. Hung, S. Sun, D. Wang, Y. Li, S. Jiang, Z. Chen, Probing the surface hydration of nonfouling zwitterionic and PEG materials in contact with proteins, ACS Appl. Mater. Interfaces 7 (2015) 16881–16888.
[21] I. Lee, K. Kobayashi, H. Sun, S. Takatani, L. Zhong, Biomembrane mimetic polymer poly (2–methacryloyloxyethyl phosphorylcholine-co-n-butyl methacrylate) at the interface of polyurethane surfaces, J. Biomed. Mater. Res. - A 82 (2007) 316–322.
[22] Z. Zhang, T. Chao, S. Chen, S. Jiang, Superlow fouling sulfobetaine and carboxybetaine polymers on glass slides, Langmuir 22 (2006) 10072–10077.
[23] H.-W. Chien, P.-H. Cheng, S.-Y. Chen, J. Yu, W.-B. Tsai, Low-fouling and functional poly (carboxybetaine) coating via a photo-crosslinking process, Biomater. Sci. 5 (2017) 523–531.
[24] C. Leng, X. Han, Q. Shao, Y. Zhu, Y. Li, S. Jiang, Z. Chen, In situ probing of the surface hydration of zwitterionic polymer brushes: structural and environmental effects, J. Phys. Chem. C 118 (2014) 15840–15845.
[25] J. Hunger, N. Ottosson, K. Mazur, M. Bonn, H.J. Bakker, Water-mediated interactions between trimethylamine-N-oxide and urea, Phys. Chem. Chem. Phys. 17 (2015) 298–306.
[26] H. Huang, C. Zhang, R. Crisci, T. Lu, H.-C. Hung, M.S.J. Sajib, P. Sarker, J. Ma, T. Wei, S. Jiang, Strong surface hydration and salt resistant mechanism of a new nonfouling zwitterionic polymer based on protein stabilizer TMAO, J. Am. Chem. Soc. 143 (2021) 16786–16795.
[27] T. Wei, M.S.J. Sajib, M. Samieegohar, H. Ma, K. Shing, Self-Assembled Monolayers of an Azobenzene Derivative on Silica and Their Interactions with Lysozyme, Langmuir 31 (2015) 13543–13552.
[28] T. Wei, M.A. Carignano, I. Szleifer, Lysozyme adsorption on polyethylene surfaces: why are long simulations needed? Langmuir 27 (2011) 12074–12081.
[29] T. Wei, M.A. Carignano, I. Szleifer, Molecular dynamics simulation of lysozyme adsorption/desorption on hydrophobic surfaces, J. Phys. Chem. B 116 (2012) 10189–10194.
[30] T. Wei, L. Zhang, H. Zhao, H. Ma, M.S.J. Sajib, H. Jiang, S. Murad, Aromatic polyamide reverse-osmosis membrane: an atomistic molecular dynamics simulation, J. Phys. Chem. B 120 (2016) 10311–10318.
[31] T. Wei, T. Huang, B. Qiao, M. Zhang, H. Ma, L. Zhang, Structures, Dynamics, and Water Permeation Free Energy across Bilayers of Lipid A and Its Analog Studied with Molecular Dynamics Simulation, J. Phys. Chem. B 118 (2014) 13202–13209.

[32] M.J. Penna, M. Mijajlovic, M.J. Biggs, Molecular-level understanding of protein adsorption at the interface between water and a strongly interacting uncharged solid surface, J. Am. Chem. Soc. 136 (2014) 5323–5331.
[33] J. Liu, J. Zhou, Hydrolysis-controlled protein adsorption and antifouling behaviors of mixed charged self-assembled monolayer: a molecular simulation study, Acta Biomater. 40 (2016) 23–30.
[34] X. Quan, J. Liu, J. Zhou, Multiscale modeling and simulations of protein adsorption: progresses and perspectives, Curr. Opin. Colloid Interface Sci. 41 (2019) 74–85.
[35] Y. Xiang, R.-G. Xu, Y. Leng, Molecular simulations of the hydration behavior of a zwitterion brush array and its antifouling property in an aqueous environment, Langmuir 34 (2018) 2245–2257.
[36] Q. Shao, Y. He, A.D. White, S. Jiang, Difference in hydration between carboxybetaine and sulfobetaine, J. Phys. Chem. B 114 (2010) 16625–16631.
[37] Q. Shao, Y. He, S. Jiang, Molecular dynamics simulation study of ion interactions with zwitterions, J. Phys. Chem. B 115 (2011) 8358–8363.
[38] P. Ganguly, J. Polák, N.F. van der Vegt, J. Heyda, J.-E. Shea, Protein stability in TMAO and mixed urea–TMAO solutions, J. Phys. Chem. B 124 (2020) 6181–6197.
[39] H. Wei, Y. Fan, Y.Q. Gao, Effects of urea, tetramethyl urea, and trimethylamine N-oxide on aqueous solution structure and solvation of protein backbones: a molecular dynamics simulation study, J. Phys. Chem. B 114 (2010) 557–568.
[40] A. Rani, A. Jayaraj, B. Jayaram, V. Pannuru, Trimethylamine-N-oxide switches from stabilizing nature: a mechanistic outlook through experimental techniques and molecular dynamics simulation, Sci. Rep. 6 (2016) 23656.
[41] D.R. Canchi, P. Jayasimha, D.C. Rau, G.I. Makhatadze, A.E. Garcia, Molecular mechanism for the preferential exclusion of TMAO from protein surfaces, J. Phys. Chem. B 116 (2012) 12095–12104.
[42] T. Zhang, T. Wei, Y. Han, H. Ma, M. Samieegohar, P.-W. Chen, I. Lian, Y.-H. Lo, Protein–ligand interaction detection with a novel method of transient induced molecular electronic spectroscopy (TIMES): experimental and theoretical studies, ACS Cent. Sci. 2 (2016) 834–842.
[43] M.S. Jahan Sajib, P. Sarker, Y. Wei, X. Tao, T. Wei, Protein corona on gold nanoparticles studied with coarse-grained simulations, Langmuir 36 (2020) 13356–13363.
[44] H. Mohanram, A. Kumar, C.S. Verma, K. Pervushin, A. Miserez, Three-dimensional structure of Megabalanus rosa Cement Protein 20 revealed by multi-dimensional NMR and molecular dynamics simulations, Philos. Trans. R. Soc. B Biol. Sci. 374 (2019), 20190198.
[45] A. Kumar, H. Mohanram, J. Li, H. Le Ferrand, C.S. Verma, A. Miserez, Disorder–order interplay of a barnacle cement protein triggered by interactions with calcium and carbonate ions: a molecular dynamics study, Chem. Mater. 32 (2020) 8845–8859.
[46] M.J. Abraham, T. Murtola, R. Schulz, S. Páll, J.C. Smith, B. Hess, E. Lindahl, GROMACS: High performance molecular simulations through multi-level parallelism from laptops to supercomputers, SoftwareX 1-2 (2015) 19–25.
[47] J. Huang, S. Rauscher, G. Nawrocki, T. Ran, M. Feig, B.L. De Groot, H. Grubmüller, A.D. MacKerell, CHARMM36m: an improved force field for folded and intrinsically disordered proteins, Nat. Methods 14 (2017) 71–73.
[48] S.V. Patwardhan, F.S. Emami, R.J. Berry, S.E. Jones, R.R. Naik, O. Deschaume, H. Heinz, C.C. Perry, Chemistry of aqueous silica nanoparticle surfaces and the mechanism of selective peptide adsorption, J. Am. Chem. Soc. 134 (2012) 6244–6256.
[49] G. Bussi, D. Donadio, M. Parrinello, Canonical sampling through velocity rescaling, J. Chem. Phys. 126 (2007), 014101.
[50] B. Isralewitz, M. Gao, K. Schulten, Steered molecular dynamics and mechanical functions of proteins, Curr. Opin. Struct. 11 (2001) 224–230.
[51] S. Kumar, J.M. Rosenberg, D. Bouzida, R.H. Swendsen, P.A. Kollman, The weighted histogram analysis method for free-energy calculations on biomolecules. I. The Method, J. Comput. Chem. 13 (1992) 1011–1021.
[52] S. Zheng, M.S.J. Sajib, Y. Wei, T. Wei, Discontinuous molecular dynamics simulations of biomolecule interfacial behavior: study of ovispirin-1 adsorption on a graphene surface, J. Chem. Theory Comput. 17 (2021) 1874–1882.
[53] P. Sarker, M.S.J. Sajib, X. Tao, T. Wei, Multiscale simulation of protein corona formation on silver nanoparticles: study of ovispirin-1 peptide adsorption, J. Phys. Chem. B 126 (2022) 601–608.
[54] F. Merzel, J.C. Smith, Is the first hydration shell of lysozyme of higher density than bulk water? Proc. Natl. Acad. Sci. USA 99 (2002) 5378–5383.
[55] S.-W. Hung, P.-Y. Hsiao, C.-C. Chieng, Dynamic information for cardiotoxin protein desorption from a methyl-terminated self-assembled monolayer using steered molecular dynamics simulation, J. Chem. Phys. 134 (2011), 194705.
[56] M. Samieegohar, H. Ma, F. Sha, M.S. Jahan Sajib, G.I. Guerrero-García, T. Wei, Understanding the interfacial behavior of lysozyme on Au (111) surfaces with multiscale simulations, Appl. Phys. Lett. 110 (2017), 073703.
[57] Z. Zhang, T. Wu, Q. Wang, H. Pan, R. Tang, Impact of interfacial high-density water layer on accurate estimation of adsorption free energy by Jarzynski's equality, J. Chem. Phys. 140 (2014), 034706.
[58] M. Rezaeisadat, N. Salehi, A.-K. Bordbar, Inclusion of levodopa into β-cyclodextrin: a comprehensive computational study, ACS Omega 6 (2021) 23814–23825.
[59] B. Chen, Z. Kang, C. Yao, B. Zhang, Y. Liu, Q. Wang, De-shielding of activatable cell-penetrating peptides: recognizing and releasing in activation process, Res. Chem. Intermed. 47 (2021) 117–130.
[60] Y. Chen, S.-C. Luo, Synergistic effects of ions and surface potentials on antifouling poly (3, 4-ethylenedioxythiophene): comparison of oligo (ethylene glycol) and phosphorylcholine, Langmuir 35 (2019) 1199–1210.
[61] M. Dogangun, P.E. Ohno, D. Liang, A.C. McGeachy, A.G. Be, N. Dalchand, T. Li, Q. Cui, F.M. Geiger, Hydrogen-bond networks near supported lipid bilayers from vibrational sum frequency generation experiments and atomistic simulations, J. Phys. Chem. B 122 (2018) 4870–4879.
[62] W.J. Yang, T. Cai, K.-G. Neoh, E.-T. Kang, S.L.-M. Teo, D. Rittschof, Barnacle cement as surface anchor for "clicking" of antifouling and antimicrobial polymer brushes on stainless steel, Biomacromolecules 14 (2013) 2041–2051.